IS MAGNETIC PINNING A DOMINANT MECHANISM IN NB-TI?

L. D. Cooley †, P. J. Lee †, and D. C. Larbalestier*†
†Applied Superconductivity Center
* Department of Materials Science and Engineering
University of Wisconsin-Madison
1500 Johnson Drive
Madison, WI 53706

Abstract

We have compared the pinning behavior of an artificial pinning center (APC) composite and a nanometer-filament Nb 46.5 wt% Ti composite to that of a conventional Nb 48 wt% Ti composite. The microstructure of the APC composite resembles the conventional composite, where ribbons of normal metal form the pinning centers, whereas the nanometer-filament composite has no internal normal metal but pins instead at the filament surface. The APC composite exhibits much stronger pinning relative to B_{c_2} than the conventional composite (21.4 GN/m^3, 7 T vs. 18.9 GN/m^3, 11 T), which is possibly due to the increased amount of pinning center (50 vol.% vs. 25 vol.%), however the proximity effect reduces the B_{c_2} unfavorably. In all three composites, F_p was proportional to $(1-b)^{3/2}$, which suggests that the magnetic interaction, rather than core pinning, dominates. Moreover, F_p obeyed a scaling relation as T tends to T_c in the conventional composite, and over a wide range of temperature in the APC composite. In these regimes, one pinning body is also dominant, where pinning done by clusters of pinning centers, rather than the individual pins, is suggested.

Introduction

Recently, Meingast, Lee, and Larbalestier [1] and Meingast and Larbalestier [2] attempted to correlate the pinning mechanisms due to variations in κ ($\delta\kappa$) and H_c (δH_c) with detailed measurements of the microstructure and bulk pinning force (F_p) for a conventionally-processed Nb 48 wt% Ti composite. This composite had previously attained one of the highest F_p values ever measured for the Nb-Ti system [3], and was thought to be free from extrinsic limitations (such as sausaging), making it well-suited for a flux pinning study. The maximum value of F_p was obtained when the α -Ti precipitates were about 1 nm thick, much less than the coherence length ($\xi(T=0) \approx 4.7$nm). Also, a large number of precipitates were observed to form in clusters, in which the average separation of the precipitates decreased to 1–2 nm from the bulk average of $\sim$ 5 nm. Because the integral expression for the Ginzburg-Landau free energy has a length scale no shorter than ξ, it was suggested that pinning by the clusters of precipitates should be considered, in addition to the effects of individual precipitates, in determining the pinning mechanisms. κ and H_c were then thought to take on values appropriate for the average composition of the precipitate cluster, whereby δH_c would become greatly enhanced as T tended to T_c. The observation of the non-scaling of F_p as $t \equiv T/T_c$ increased from 0.25 to 0.75 was then explained by the fact that both $\delta\kappa$ and δH_c were strong, whereas scaling of F_p at $t = 0.98$ was in agreement with the domination of δH_c there. Unfortunately, the proportionality of F_p to $(1-b)^{3/2}$ in the latter case was unexpected, since δH_c should vary as $(1-b)$. This data is shown in figure 1. Similar scaling/non-scaling behavior has been reported by Matsushita and Küpfer, [4, 5] and the very recent results of McKinnell [6] show that this behavior occurs in Nb-Ti alloys throughout their useful composition range (from about 44 to 62 wt% Ti).

In this paper, we compare the microstructural and flux pinning characteristics of two different composites, both of which exhibit the $(1-b)^{3/2}$ scaling behavior, with the conventional composite above. The first composite is a submicron-filament Nb 46.5 wt% Ti composite in a copper stabilizer, which was manufactured without heat treatment, similar to the composite investigated by Hlasnik, et. al. [8] The experimental results will not be reported in detail here—the pinning force curve is shown in figure 2. The second composite is an artificial pinning center (APC) composite. APC composites involve a new processing technique, [9, 10, 11] where the pinning center is introduced as a starting component in the interior of the superconductor, instead of relying on "natural" formation methods such as precipitation or reaction. This allows, in the ideal case, the pinning center microstructure to exactly match the fluxon lattice for some field and temperature. Strong pinning forces should then be created.

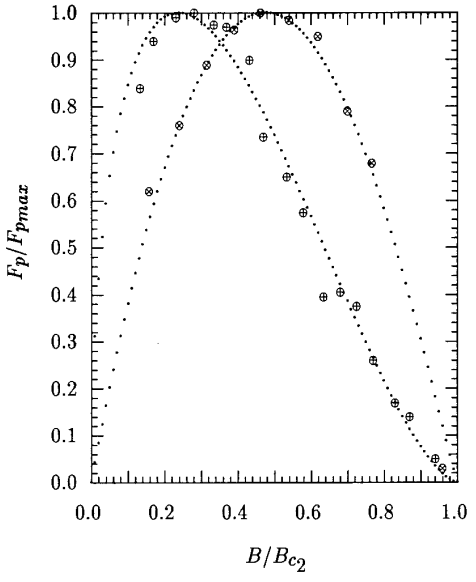

Figure 1: Reduced bulk pinning force vs. reduced field for a conventional Nb 48 wt% Ti composite (see text), at T/T_c = 0.46 ($\otimes$), and 0.98 ($\oplus$). Fits of $b^{0.9}(1-b)^{1.1}$ and $b^{0.5}(1-b)^{1.5}$ are also plotted, respectively (data taken from ref. 2).

Manuscript received September 24, 1990.

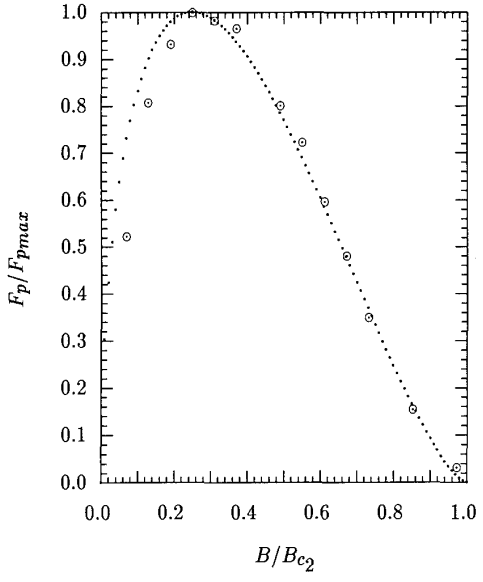

Figure 2: Reduced bulk pinning force plotted vs. reduced field for a Nb 46.5 wt% Ti composite with the filament diameter is 48 nm. A $b^{1/2}(1-b)^{3/2}$ curve is also plotted.

The composite we used was fabricated by Intermagnetics General Corporation using Nb 46.5 wt% Ti superconductor with Nb pinning centers. This composite has been the focus of previous work. [12] Interestingly, the Nb was external to the Nb-Ti at starting size in this composite, where, of course, the fluxons would not exist. However, as we will show, the microstructure of the final size composite rather resembles that of a conventional composite.

Experimental results for the APC composite

We report here the microstructural and electromagnetic measurements on the APC composite. The microstructural characterization was performed by transmission electron microscopy (TEM), using techniques described elsewhere. [13] The critical temperature was measured by a d.c. flux expulsion technique using a vibrating sample magnetometer (VSM). Flux pinning characterization was obtained from transport J_c measurements and VSM measurements of the magnetization. The transport J_c measurements were performed with the sample immersed in a bath of liquid helium, while the VSM measurements were carried out in a variable-temperature dewar which allowed the sample temperature to be varied from 2 K to above T_c. The Bean model [14] was used to obtain the critical current.

Microstructural results

Figure 3 compares TEM micrographs of the APC composite and a conventional Nb 48 wt% Ti composite at final size. [1,2] It is clear that the pinning centers, Nb in the APC composite and α -Ti in the conventional composite, are ribbon-like in cross-section for both composites. In fact, a very striking feature of the two micrographs is their apparent similarity, in spite of their very different genesis. Recall that the continuous phase in the conventional composite is the Nb-Ti and the discrete Ti-rich precipitates are produced by multiple precipitation and drawing sequences. In the APC composite the continuous phase at starting size is the deliberately-introduced Nb pinning center. Although added as a co-axial annulus around each Nb-Ti filament, [10,12] the filament structure has in fact greatly distorted during manufacture such that both microstructures share many similarities. The important difference is that there is about 18 volume % of pinning center in the conventional composite and 50 volume % in the APC composite.

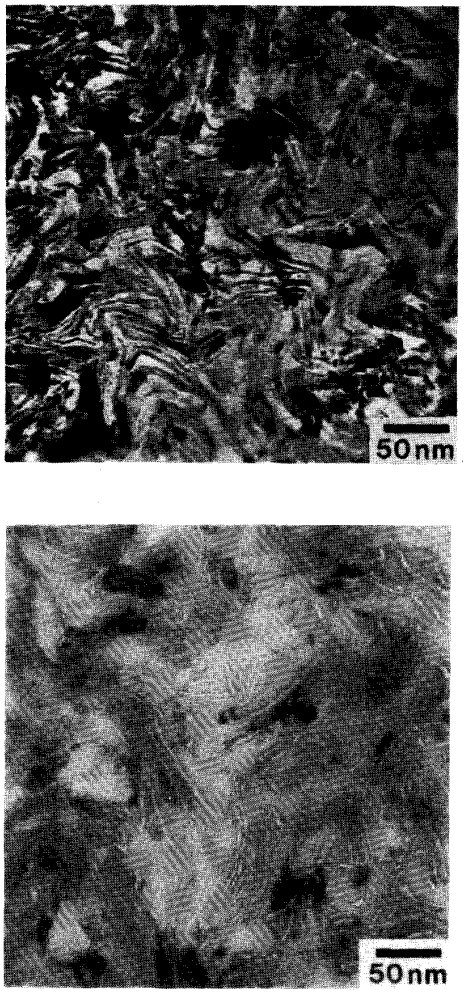

Figure 3: TEM micrographs of the APC composite (top) and a conventionally-processed Nb 48 wt% Ti composite. In the APC composite, the Nb pinning centers are the darker phase, while in the conventional composite, the α -Ti pinning centers appear as the lighter phase.

More detailed analysis of the two microstructures does show additional important differences. The APC composite appears to have significantly fewer regions which have a below average density of pins. The average thickness and spacing of the pinning centers are about 5 and 10 nm respectively in the APC composite, while the average thickness and spacing of the α -Ti

precipitates in the conventional composite are about 2 and 5 nm, respectively. Both TEM samples were taken at wires sizes which exhibited the strongest bulk pinning forces; the filament diameter for the APC composite is 8.15 μm.

Electromagnetic results

Figure 4 shows the dependence of B_{c_2} on temperature, where B_{c_2} is determined by the field at which the magnetization loop, measured in perpendicular field, closes. The extrapolation of the B_{c_2}-T curve near T_c crosses the temperature axis at 9.5 K, in agreement with the T_c of 9.51 K measured by flux expulsion. The values of $B_{c_2}(T)$, 7 tesla at 4.2 K for example, are much lower than for conventional Nb-Ti composites, where typically B_{c_2} exceeds 10 tesla at 4.2 K.

The reduced bulk pinning force vs. reduced field, as determined from the magnetization hysteresis loops, is shown in figure 5 for temperatures from 2–9 K. The extrapolation of the F_p curves (not shown) through the field axis give values of B_{c_2} which agree with those determined by the magnetization loop closure within 2 % . A least-squares iterative fit to the data in figure 5 gives F_p proportional to $b^{0.9}(1-b)^{1.6}$ at 2.1 K, changing slightly to $b(1-b)^{1.5}$ for higher temperatures. The bulk pinning force is plotted against B_{c_2} in figure 6 for values of $b \equiv B/B_{c_2}$ of 0.2, 0.5, and 0.8. The slope of a fit by hand to the data gives a variation in the exponent of B_{c_2}, where F_p is proportional to $B_{c_2}^n$, of 2.45–2.51. By contrast, the exponent varied from 1.82 to 2.29 in the conventional composite.

Discussion

Pinning in the ideal APC composite

In an ideal Nb-Ti APC composite, the pinning centers could be made to be $2\xi(T)$ thick and $a_0(B)$ in center-to-center separation. Depending on T and B, these parameters can vary from about 10–35 nm and 200–10 nm respectively for increasing temperature and field. Let us consider the case which is applicable to the APC composite: we take the thickness and separation of the pinning centers to be much less than ξ. In this case, the proximity effect operates throughout, such that the local superconducting parameters are effectively averaged over a volume proportional to ξ^3. The gap and order parameter vary only weakly throughout the composite, therefore H_c and κ are virtually constant everywhere. The free energy will then be practically constant everywhere, due to the uniform spacing and thickness of the pinning centers. The elementary pinning mechanisms also suffer averaging effects, and a dominant mechanism will control F_p only if we relax the presumption of uniform spacing and separation of the pinning centers. This could describe the case observed by Meingast and Larbalestier [2] for temperatures near T_c.

Discussion of the experimental results

The size and spacing of the pinning centers determined from the micrograph of the APC composite are both approximately 2–5 nm. From the measured values of B_{c_2}, ξ is 5–20 nm, which places the composite in the regime discussed above. The average composition of the APC composite is Nb 18.8 wt% Ti. The observed values of B_{c_2} and T_c agree with published [17] values for a Nb-Ti alloy with this composition. Also, the measured value of dB_{c_2}/dT at T_c of -1.35 T/K is close to that of -1.5 T/K measured by Muller[18] for a 70 at% Nb alloy. The hypothesis that the proximity effect is everywhere dominant is, then, supported.

The data presented in figures 5, 6, and 7 can be combined to get a scaling relation for F_p:

$$F_p = 2.2 \times 10^{12} B_{c_2}^{5/2}(T) d^{2/3} b(1-b)^{3/2} \ [\mathrm{N/m^3}], \qquad (1)$$

where d is the filament diameter. The deviation of the field

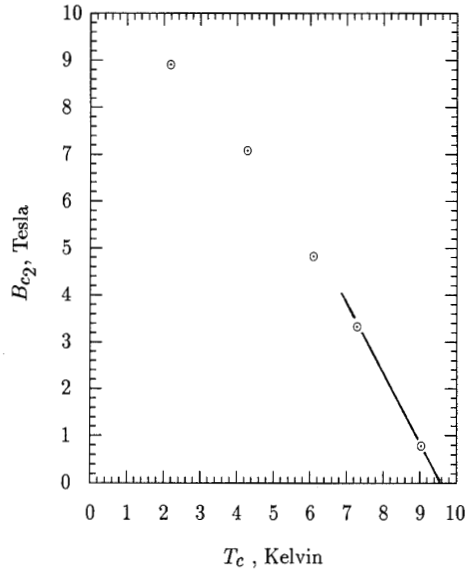

Figure 4: The upper critical field, determined by the closure of the magnetization loop, vs. critical temperature for the APC composite.

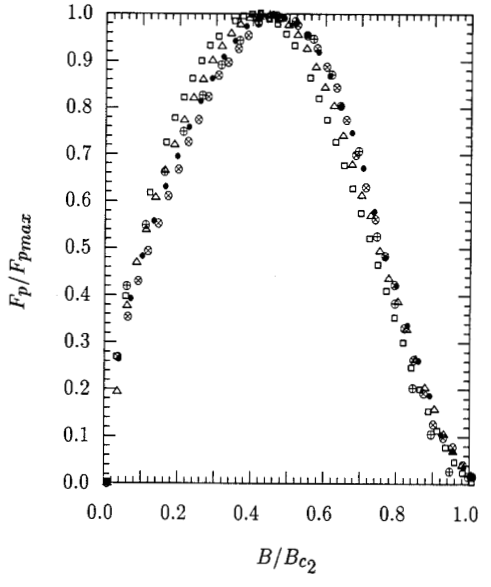

Figure 5: The reduced bulk pinning force versus the reduced flux density, for reduced temperatures of 0.22 (□), 0.44 (△), 0.63 (•), 0.75 (⊗), and 0.93 (⊕) for the APC composite.

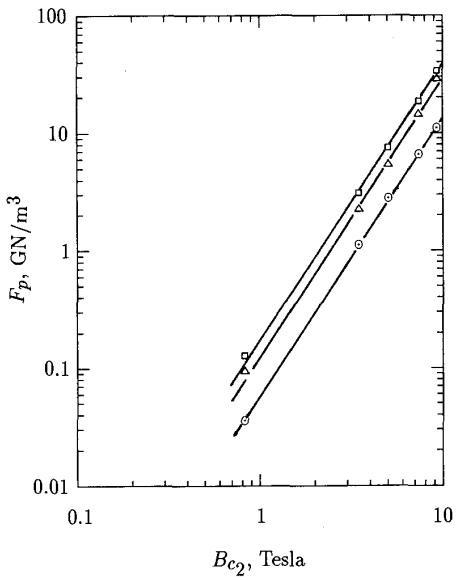

Figure 6: The bulk pinning force versus the upper critical field, for reduced fields (B/B_{c_2}) of 0.2 (△), 0.5 (□), and 0.8 (⊙) for the APC composite. The slope of the lines fitted by hand varies from 2.45 to 2.51.

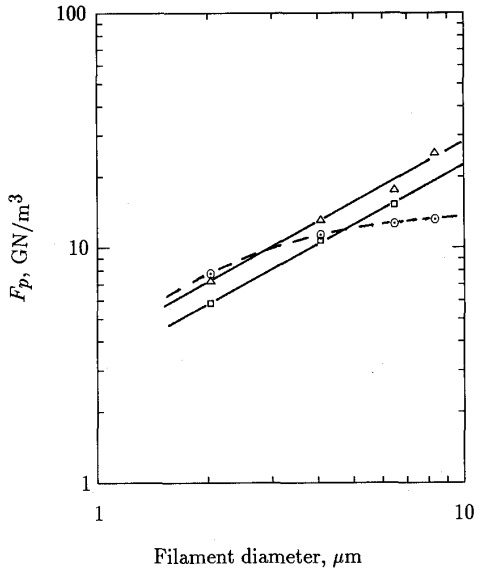

Figure 7: The bulk pinning force versus the filament diameter, for reduced temperature = 0.44 and at reduced fields of 0.28 (□), 0.43 (△), and 0.71 (⊙), for the APC composite.

dependence scaling of F_p at low temperatures may be due to individual pinning centers contributing to the overall pinning, since $\xi(2.1K) = 6$ nm is then about equal to the thickness and spacing of the pinning centers. Also, the filament diameter scaling becomes less good as data from higher fields is used. This is due to the increasing influence of filament instabilities (sausaging) on the transport J_c data, from which the filament diameter dependence was obtained. For the most part, however, the scaling applies. The bulk pinning forces predicted by this equation are very strong: the measured value of F_{pmax}/B_{c_2} for the APC composite is almost double that for a conventional composite (21.4 GN/m^3, 7 T vs. 18.9 GN/m^3, 10.5 T). This result is a further data point supporting the linear dependence of F_p on volume % pinning center previously established by Lee, McKinnell, and Larbalestier. [19] Unlike conventional composites, where the pinning center volume cannot easily exceed 25 %, the APC composite contains about 50 vol% of normal metal, as mentioned.

Since the Nb clusters appear to be the dominant pinning center, the fact that a scaling relation is found suggests that one pinning mechanism is dominant. Yet, the $(1-b)^{3/2}$ factor in the F_p field dependence is unexpected—the $\delta\kappa$ and δH_c pinning mechanisms should have only a $(1-b)$ dependence, while in the case of fluxon shear a $(1-b)^2$ dependence is expected. [20] This factor has, as mentioned, been reported for the scaling relation observed in a conventional Nb 48 wt% Ti composite [2] for T close to T_c, as shown in figure 1, and has also been observed for a submicron-filament Nb 46.5 wt% Ti composite processed without heat treatment, as shown in figure 2. The latter composite also achieved very strong bulk pinning forces, 22 GN/m^3 at 2 tesla, 4.2 K, as determined by transport J_c measurement. [21] The pinning in that composite can only be due to the magnetic interaction of the fluxons with the filaments' surfaces, according to the theory of Takács [22], since there are no other defects of large enough density to be effective.

These factors of $(1-b)^{3/2}$ are intriguing, since historically the preponderance of opinion has been that optimized, strong-pinning Nb-Ti pins according to a $(1-b)$ factor. One mechanism that is suggested is the magnetic interaction. This interaction is determined by the shielding current and the vector potential of the fluxon, which are proportional to the depairing current density, J_d. The expression for the field-dependent depairing current is [23]

$$J_d = 0.54\frac{H_c}{\lambda}(1-b)^{3/2}, \tag{2}$$

which may explain the field dependence of F_p.

It is not clear how the pinning clusters could create a magnetic pinning interaction, since only the δH_c and $\delta\kappa$ interactions are expected far from the surface of the filament. One possibility is that the proximity effect may cause the entire pinning cluster to have a depressed or even zero order parameter. Such regions are large compared to ξ or a_0 and therefore can pin strongly through the magnetic interaction. [15, 16] We can express the free energy perturbation due to the magnetic interaction as

$$\delta F = \int dV \frac{\partial F}{\partial A}\delta A = \int dV \mu_0 J_s A \frac{\delta A}{A}, \tag{3}$$

where A is the vector potential and J_s is the shielding current around a fluxon. Eqation (4) is proportional to $b(1-b)^{3/2}$, since the shielding current is proportional to J_d. The magnitude of the energy perturbation is on the order of $\mu_0 H_c^2$, since A is proportional to λH_c and J_s is proportional to $\mu_0 H_c/\lambda$, thus strong pinning is expected.

Conclusions

In summary, we have compared the pinning of an optimally-processed conventional composite (18 vol.% precipitate), an APC composite (50 vol.% pinning center), and a nanometer-filament composite which has no pinning centers but pins instead at the filament surface. The APC composite exhibits much stronger pinning relative to B_{c_2} than the conventional composite, which is possibly due to the increased amount of pinning center, however the proximity effect reduces the B_{c_2} unfavorably. In all three composites, F_p was proportional to $(1-b)^{3/2}$, which suggests that the magnetic interaction, rather than core pinning, dominates. Moreover, F_p obeyed a scaling relation as T tends to T_c in the conventional composite, and over a wide range of temperature in the APC composite. One pinning body is then also dominant, where the attention is clearly focussed on clusters of pinning centers, rather than the individual pins.

Acknowledgements

We would like to thank L. Motowidlo and B. Zeitlin of Intermagnetics General Corporation who provided us with the APC composite samples. This work is supported by the Department of Energy, High Energy Physics Fund.

References

[1] C. Meingast, P. J. Lee, and D. C. Larbalestier. *Journal of Applied Physics* 66 (12), 5962 (1989).

[2] C. Meingast and D. C. Larbalestier. *Journal of Applied Physics* 66 (12), 5971 (1989).

[3] C. Li and D. C. Larbalestier. *Cryogenics* 27, 171 (1987).

[4] T. Matsushita and H. Küpfer. *Journal of Applied Physics* 63, 5048 (1988).

[5] H. Küpfer and T. Matsushita. *Journal of Applied Physics* 63, 5060 (1988).

[6] J. C. McKinnell. "Flux Pinning in Superconducting Nb-Ti Alloys." Ph. D. Thesis, University of Wisconsin-Madison, Madison, WI. May, 1990.

[7] C. Meingast et. al. *Applied Physics Letters* 51 (9), 688 (1987).

[8] I. Hlasnik et. al. *Cryogenics* 25, 558 (1985).

[9] G. L. Dorofejev et. al. In "Proceedings of the International Conference on Magnet Technology," Zurich, Switzerland (1985), p. 564. (Swiss Inst. for Nuc. Res.).

[10] B. A. Zeitlin, M. S. Walker, and L. R. Motowidlo. United States Patent number 4,803,310. February 7, 1989.

[11] M. Klemm et. al. *Superconductor Science and Technology* 3 (5), 249 (1990).

[12] L. R. Motowidlo, H. C. Kanithi, and B. A. Zeitlin. *Advances in Cryogenic Engineering (Materials)* 36A, 311 (1990).

[13] P. J. Lee and D. C. Larbalestier. *Journal of Materials Science* 23, 3951 (1988); P. J. Lee and D. C. Larbalestier. *Acta Metallurgica* 35 (10) 2523 (1987).

[14] C. P. Bean. *Reviews of Modern Physics* 36, 31 (1964).

[15] A. M. Campbell and J. E. Evetts. *Advandes in Physics* 21, 199 (1972).

[16] H. Ullmaier. *Irreversible Properties of Type II Superconductors*, volume 76 of "Springer Tracts in Modern Physics." Springer Verlag, Berlin, FRG, 1975.

[17] D. C. Larbalestier. "Niobium-titanium superconducting materials." In S. Foner and B. B. Schwartz, editors, *Superconductor Materials Science,* page 133. Plenum Press, New York, NY, 1981.

[18] H. J. Muller. "The Upper Critical Field of Niobium-Titanium." Ph. D. Thesis, University of Wisconsin-Madison, Madison, WI. January, 1989.

[19] P. J. Lee, J. C. McKinnell, and D. C. Larbalestier. *Advances in Cryogenic Engineering (Materials)* 35A, 287 (1990).

[20] E. H. Brandt. *Physical Review* B34, 6514 (1986).

[21] L. D. Cooley and D. C. Larbalestier. Unpublished, 1989.

[22] S. Takács. *Czech. J. Phys.,* B36, 524 (1986).

[23] R. G. Boyd. *Physical Review,* 145 (1), 255 (1966).